tvst

Article

Development of Primary Open Angle Glaucoma-Like Features in a Rhesus Macaque Colony From Southern China

Louis R. Pasquale[1], Li Gong[2], Janey L. Wiggs[3], Lingzhen Pan[2], Zhenyan Yang[2], Mingling Wu[2], Zunyuan Yang[2], Dong Feng Chen[3], and Wen Zeng[2]

[1] Eye and Vision Research Institute of New York Eye and Ear at Mount Sinai, Mount Sinai Icahn School of Medicine, New York, NY, USA
[2] PriMed Non-human Primate Research Center of Sichuan PriMed Shines Bio-tech Co., Ltd., Ya'an, Sichuan Province, China
[3] Massachusetts Eye and Ear, Department of Ophthalmology, Harvard Medical School, Boston, MA, USA

Correspondence: Wen Zeng, PriMed Non-Human Primate Research Center of Sichuan PriMed Shines Bio-tech Co., Ltd., Ya'an, Sichuan Province 625000, China.
e-mail: zengwen@scprimed.com
Dong Feng Chen, Schepens Eye Research Institute of Massachusetts Eye and Ear, Department of Ophthalmology, Harvard Medical School, Boston, MA 02114, USA.
e-mail: dongfeng_chen@meei.harvard.edu

Received: March 18, 2021
Accepted: June 2, 2021
Published: August 17, 2021

Keywords: rhesus monkeys; primary open-angle glaucoma; intraocular pressure; cup disc ratio; retinal nerve fiber layer; spectrum domain-optical coherence tomography

Citation: Pasquale LR, Gong L, Wiggs JL, Pan L, Yang Z, Wu M, Yang Z, Chen DF, Zeng W. Development of primary open angle glaucoma-like features in a rhesus macaque colony from Southern China. Transl Vis Sci Technol. 2021;10(9):20, https://doi.org/10.1167/tvst.10.9.20

Purpose: To describe the ocular phenotype of spontaneous glaucoma in a non-human primate colony.

Methods: In total, 722 Rhesus macaque monkeys aged 10 to 25 years underwent optical coherence tomography (OCT), fundus photography (FP), and intraocular pressure (IOP) measurements. Monkeys with baseline cup-to-disc ratio (CDR) <0.5 were used to establish baseline ocular features. A subset was followed longitudinally for three years and compared to glaucoma suspects on the basis of OCT/FP criteria.

Results: The average IOP under ketamine sedation and average CDR for the entire colony was 13.0 ± 4.3 mm Hg and 0.38 ± 0.07, respectively. The mean baseline conscious IOP of glaucoma suspects ($N = 18$) versus controls ($N = 108$) was 16.2 ± 3.5 mm Hg and 13.9 ± 2.3 mm Hg, respectively ($P = 0.001$). All glaucoma suspects had unremarkable slit lamp examinations and open angles based on anterior segment OCT. Baseline global circumpapillary retinal nerve fiber layer (RNFL) thickness was 91.5 ± 11.0 µM versus 102.7 ± 8.5 µM in suspects and controls, respectively ($P < 0.0001$). All sectors on the baseline circumpapillary OCT showed a significant reduction in RNFL thickness versus controls ($P \leq 0.0022$) except for the temporal sector ($P \geq 0.07$). In three-year longitudinal analysis, neither CDR nor OCT parameters changed in controls ($N = 40$; $P \geq 0.16$), whereas significant increase in CDR ($P = 0.018$) and nominally significant decreases in two OCT sectors (nasal, $P = 0.023$ and nasal inferior, $P = 0.046$) were noted in suspects.

Conclusions: Members of a nonhuman primate colony exhibit important ophthalmic features of human primary open-angle glaucoma.

Translational Relevance: Identification of a spontaneous model of glaucoma in nonhuman primates represents an unprecedented opportunity to elucidate the natural history, pathogenesis and effective therapeutic strategies for the disease.

Introduction

Primary open-angle glaucoma (POAG) is an optic neuropathy without intraocular pressure (IOP) criteria that has been challenging to define with objective metrics.[1] Furthermore, there are few glimpses into the untreated natural history of the disease[2–4] or any understanding of its preclinical phase. Access to tissues or intraocular fluids from early untreated glaucoma is rarely, if ever, available.

There are several iatrogenic and genetic models of glaucoma in rodents to study the glaucomatous process.[5] Although rodent models of glaucoma offer many advantages, including providing insight into human glaucoma, they are distantly related to humans;

thus the results obtained from these models may not always reflect human pathogenesis. Moreover, the disease models are frequently induced by a single insult such as episcleral vein ablation,[6] drainage angle occlusion with microbeads,[7] trabecular meshwork dysfunction with glucocorticoid exposure,[8] temporary anterior chamber pressurization,[9] or single gene alterations such as *MYOC* mutations,[10,11] which may not fully capture the complexity of POAG pathogenesis. There are also nonhuman primate models of glaucoma caused by various interventions that have been useful to understand how increased IOP affects the optic nerve.[12] However, disease models often have distinct molecular pathophysiology from spontaneously developed disease, which might explain the poor translation of many neuroprotective strategies from preclinical to clinical trials. The larger nonhuman primate eye with anterior chamber and vitreous volumes more comparable to the human eye affords more opportunities to translate new interventions into humans but offers its own challenges. A macaque colony from the Caribbean developed spontaneous open-angle glaucoma across a range of IOP[13]; however, this model has not been studied in great detail. To date, there is a paucity of literature reporting a spontaneously developed glaucomatous model in non-human primates.

In this study we describe the ocular features of a rhesus macaque monkey cohort that is part of a large captive colony in Ya'an, southern China. Some of these monkeys develop a host of diseases comparable to human complex conditions such as age-related macular degeneration, diabetes mellitus, hypertension, liver disease, and hearing loss. Our data demonstrate the development of salient features of POAG in this colony.

Methods

Animals

This study adhered to the tenets of the Declaration of Helsinki and complied with the National Institutes of Health Guide for the Care and Use of Laboratory Animals and the guidelines of the Association for Research of Vision and Ophthalmology. The PriMed Non-Human Primate Research Center in Ya'an is located in southern China and is a fully Association for Assessment and Accreditation of Laboratory Animal Care (AAALAC)-accredited facility permitted to perform laboratory animal research from the Peoples Republic of China. All rhesus macaques (*M. mulatta*) were pair-housed in accordance with standard operating procedures of PriMed in a climate-controlled room at 18°C to 26°C with a relative humidity of 40% to 70% and a 12-hour light/12-hour dark cycle. The rate of ventilation was eight times/hour. Monkeys had free access to drinking water and were continually fed with monkey chow (12% calories from fat, 18% calories from protein, and 70% calories from carbohydrates) at 200 to 300 g/d. Daily allotment of fruits, vegetables, or additional supplements and various toys were also provided. All experimental protocols were reviewed and approved by the Institutional Animal Care and Use Committee of Sichuan Primed Shines Bio-tech Co., Ltd. No animals were sacrificed for the purposes of this work.

Study Design

Overall, 722 monkeys (10–25 years old; 338 males, 384 females) formed the colony at risk for glaucoma and all underwent measurement of blood pressure, various blood tests, measurement of IOP, slit lamp biomicroscopy, ocular coherence tomography (OCT) and fundus photography (FP) under sedation as described in detail below. After determining the variance in cup disc ratio (CDR) from OCT in this population (see details below), we selected 108 monkeys with values <95% confidence interval for the colony, regardless of sedated IOP levels as a control group nested within this colony at risk. Next, two ophthalmologists independently reviewed all ophthalmic data and defined glaucoma suspects based on the following optic nerve criteria: CDR>0.5 based on the OCT, focal narrowing of the neuroretinal rim based on slit biomicroscopic exam of the optic nerve, disc hemorrhage based on inspection of FPs, OCT demonstration of retinal nerve fiber layer (RNFL) defects defined as diffuse or focal sectorial thinning compared to normal ($P < 0.01$ in one OCT examination or $P < 0.05$ twice in two OCT examinations that were performed six months apart). Glaucoma suspects (15 of 18 total; three females were placed back into the breeding colony) and 40 age- and gender-matched controls were then followed with annual conscious IOP measurements and OCT over three years.

Blood Pressure Assessments

Blood pressure measurements were conducted at 2:00 pm to 4:00 pm. Monkeys were anesthetized with ketamine hydrochloride (Alfasan International B.V., Woerden, Holland) at 10 mg/kg body weight intramuscularly. Fifteen minutes after ketamine injection, monkeys were laid on a bed in a supine position. Hair on the left upper arm was shaved. A cuff connecting to a bedside monitor (GE B40i; GE-Healthcare, Chicago,

Table 1. Characteristics of Rhesus Monkeys Selected as Controls From the Colony at Risk for Glaucoma

Features	Males ($n = 70$)	Females ($n = 38$)	*P* Value
Age (years)	14.6 ± 2.2	14.7 ± 1.6	0.81
Body weight (kg)	10.8 ± 0.7	6.6 ± 0.9	<0.0001
Systolic blood pressure (mm Hg)	131.1 ± 16.6	129.1 ± 11.3	0.50
Diastolic blood pressure (mm Hg)	65.1 ± 9.8	63.8 ± 5.0	0.46
Fasting plasma glucose (mg/dL)	83.9 ± 13.8	81.3 ± 16.5	0.38
Triglycerides (mg/dL)	0.48 ± 0.15	0.50 ± 0.17	0.46
Cup disc ratio	0.37 ± 0.08	0.36 ± 0.07	0.77
Conscious IOP (mm Hg)			
OD	14.1 ± 2.3	14.0 ± 2.5	0.33
OS	14.0 ± 2.5	13.7 ± 2.1	0.51

Data are presented as mean ± standard deviation. *P* values represent comparison of females versus males.

IL, USA) was placed on the upper extremity. A series of three measurements was obtained automatically at one-minute intervals. A new set of measurements was performed if the difference between the lowest and the highest reading exceeded 15 mm Hg. Monkeys with three measures of systolic blood pressure >180 mm Hg or diastolic blood pressure >110 mm Hg were classified as having severe hypertension and treated with valsartan (Beijing Novartis Pharmaceutical Inc., Beijing, China), an angiotensin II receptor blocker.

Blood Tests

Monkeys were fasted 14 to 16 hours with free access to drinking water. Before blood collection, monkeys were anesthetized with ketamine hydrochloride (10 mg/kg body weight intramuscularly). Blood draw was conducted at 8:00 am to 9:00 am, and 1 mL of blood was collected from the saphenous vein. Biochemistry tests listed in Table 1 were performed using a Cobas6000 analyzer (Roche Diagnostics, Basel, Switzerland). Monkeys with fasting plasma glucose (FPG) > 185 mg/mL on two different days, accompanied by >10% weight loss were classified as having severe diabetes mellitus and given insulin supplement at 5 to 10 IU Lantus (insulin glargine injection; Sanofi-Aventis, Paris, France) by veterinarians on the basis of daily FPG value.

Measurements of IOP in Anesthetized Monkeys

All IOP measurements under ketamine sedation were conducted at 8:00 am to 9:00 am. Monkeys were anesthetized with ketamine hydrochloride (10 mg/kg body weight intramuscularly). One technician stabilized the monkeys in a sitting position while another technician fixed the head in primary gaze. A self-retaining eyelid speculum was placed to facilitate IOP measurements. IOP measurements were conducted by an experienced technician using an Icare tonometer (TA01i; Icare, Helsinki, Finland). The instrument automatically acquired and averaged six measurements. The mean IOP was shown on the display screen. Three series of six measurements were obtained. The measurements were excluded, if the difference between the lowest and the highest reading exceeded 3 mm Hg. The IOP values reported were the means of three series of six measurements each. The reported IOPs represent the mean of both eyes unless otherwise indicated.

Measurement of IOP in Conscious Monkeys

All measurements were carried out at 8:00 to 9:00 am. Monkeys were positioned in a chair, and a technician fixed the head in primary gaze. A self-retaining eyelid speculum was used to immobilize the eyelids, while the IOP measurements were conducted by an experienced technician using an Icare tonometer (TA01i; Icare). The technique used was similar to the procedure outlined for sedated monkeys.

FP, OCT, and Slit Lamp Biomicroscopy

Monkeys were anesthetized with ketamine/xylazine (1:1, 8 mg/kg body weight intramuscularly), and two drops of the combined tropicamide phenylephrine mydriatic agent was applied to each eye after anesthesia. Monkeys were placed in a dark room until the pupil diameter reached ≥6 mm. Monkeys were situated in a headrest, and a self-retaining eyelid speculum was placed to enable the examination. The working distance of the fundus scope was adjusted to ensure the macula and optic disc were focused clearly. Both

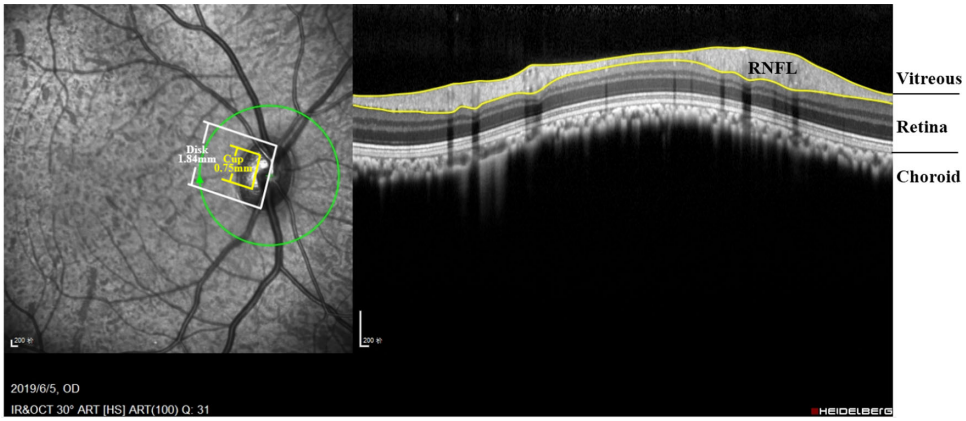

Figure 1. Spectral Domain-Optical Coherence Tomography (SD-OCT) images of optic nerve head and retinal layers in rhesus monkeys. **(A)** Representative circular circumpapillary SD-OCT image of a normal monkey showing the optic disc (*white line*) and the cup (*yellow line*). (**B**) Concentric SD-OCT scan displaying retinal cell layers of a normal eye.

macula-centered and optic disc–centered images were obtained.

Immediately after FP, an evenly illuminated, well-focused fundus image with high-quality OCT images was acquired using Heidelberg Spectralis OCT Plus (Heidelberg Engineering GmbH, Heidelberg, Germany). All OCT images had quality scores of 25 or higher. The images of optic nerve head scans were obtained by circular scans centered on the optic disc at a 3.4 mm diameter circle. Evaluation of CDR was based on the assessments of the vertical cup and disc diameters from the radiant optic disc in OCT photographs and analyzed with Spectralis OCT software version 6.9a (Fig. 1).[14] The RNFL was automatically segmented into six sectors, and the RNFL thickness was assessed automatically by the Heidelberg OCT software. The means of RNFL thickness were calculated by averaging the thickness values of 360° measures. The thickness of each sector was calculated, respectively, by averaging the measures of temporal sector (T; 315° to 45°), temporal-superior sector (TS; 45° to 90°), temporal-inferior sector (TI; 90° to 135°), nasal sector (N; 135° to 225°), nasal-superior sector (NS; 225° to 270°), and nasal-inferior sector (NI; 270° to 315°), according to manufacturer instructions. The equivalent of human chronological age (3 × monkey age) was entered into the software for the purpose of performing age matched comparisons.[15] Anterior segment OCT was performed undilated on a separate day using the Heidelberg Spectralis OCT Plus with the anterior segment module. The anterior chamber angle scan protocol was used, at an automatic real-time level of at least 50. Scans were taken at the nasal and temporal meridians, as close to the horizontal midline as possible. An open angle was defined as the absence of any contact between the iris and angle wall anterior to the scleral spur. After FP and optic nerve OCT measurements, slit lamp examination was performed. The overall structures and morphologies of the anterior segment, including eyelids, cornea, anterior chamber, lens, iris, pupil, and vitreous body, were examined.

Neuro-Imaging Studies

Post hoc we performed T1-weighted and T2 flair magnetic resonance imaging (MRI) on a male glaucoma suspect (age 16) and a male normal monkey (age 15) with a 3.0T magnet. These transverse scans focused on the chiasm, and cerebral structures were performed to rule out secondary causes for optic nerve degeneration.

Statistical Analysis

The groups were compared by paired or unpaired independent-sample *t* tests. All values are expressed as mean ± standard deviation (SD). A P value <0.05 was considered statistically significant. Because seven OCT parameters were measured, we applied a P value cutoff <0.007 to adjust for multiple comparisons.

Results

Demographic and Ocular Features of the Rhesus Monkey Colony at Risk for Glaucoma

The mean age of the 722 monkeys examined was 14.4 ± 2.0 years old. The average IOP under ketamine

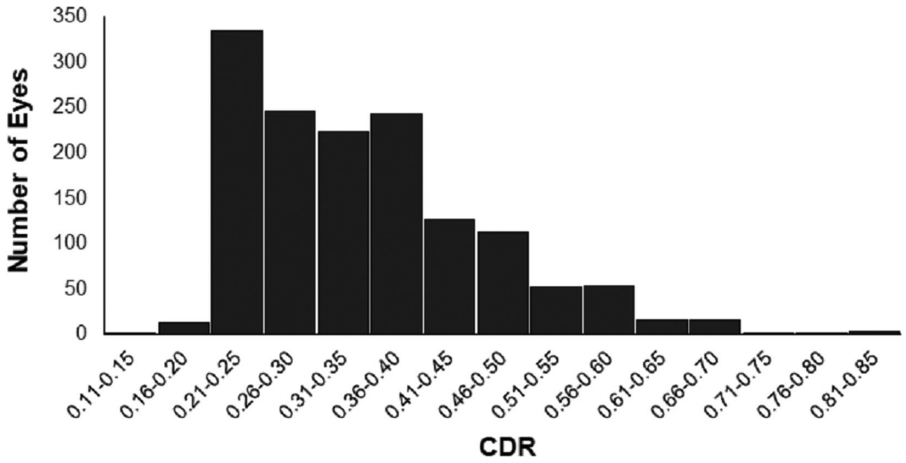

Figure 2. Distributions of CDR in Rhesus monkeys. Histogram depicting the distribution of CDR values taken from OCT images of 772 monkeys (n = 1444 eyes). The 95% confidence interval is 0.14 to 0.58.

sedation was 13.0 ± 4.3 mm Hg, with values ranging from 2 mm Hg to 27 mm Hg. The average CDR based on the useable OCT images of 1444 eyes taken from the entire 722 monkeys was 0.36 ± 0.11, with values ranging from 0.14 to 0.85 (Fig. 2). In less than 5% of the cohort, CDR value was larger than 0.5, similar to what was found in humans.[16]

Features of a Control Group Nested in the Colony at Risk for Glaucoma

To establish the normative baseline parameters in Rhesus monkeys, we randomly selected 108 normal monkeys from those with CDR < 0.5 (70 males and 38 females) regardless of sedated IOP level and with no detectable ocular and or retinal pathology on slit lamp examination and inspection of FPs. The gender-specific demographic and baseline characteristics of the 108 monkeys are outlined in Table 1. These monkeys had an average conscious IOP of 14.3 ± 2.5 mm Hg, with values ranging from 8 to 20 mm Hg (Fig. 3), and no significant differences in IOP values or other demographics, including blood pressure and FPG, were noted between male and female monkeys (Table 1). Consistent with other reports, males were significantly heavier than females.[17]

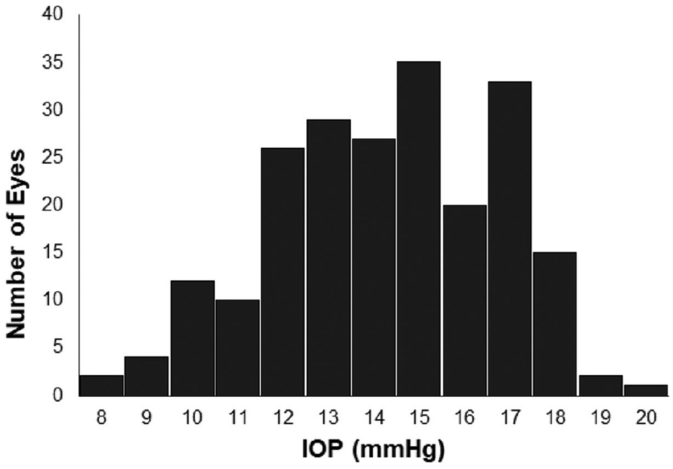

Figure 3. Distributions of IOP in Rhesus monkeys. Histograms representing the distribution of conscious IOP measured from 108 monkeys not regarded as glaucoma suspects. The 95% confidence interval is 9.3 mm Hg to 19.3 mm Hg.

The average global RNFL thickness of the control monkeys ranged from 100.9 ± 8.1 µm to 103.3 ± 8.5 µm for right and left eyes of male and female control monkeys (Table 2). We found no significant differences of RNFL thickness in any sector between left and right eyes of male and female control monkeys ($P \geq 0.15$; Table 2). An example of the OCT output from a 19-year-old female control is provided in Figure 4. The RNFL parameters of these monkeys were in agreement with the normative database and fell within the normal range of RNFL parameters of normal human subjects.[18,19]

Identification of Monkeys With Glaucoma-Like Features in the Cohort at Risk for Glaucoma

Through screening the cohort of 722 Rhesus monkeys, we identified 18 (11 males and 7 females) monkeys with at least one eye (total 31 eyes) that met the glaucoma suspect criteria detected with at least two of the following signs when independently scored by two ophthalmologists: symmetric

Table 2. RNFL Parameters by Spectral Domain-OCT for Control Monkeys

	Males (n = 70)		Females (n = 38)		*P* Value	
Parameter (μm)	OD	OS	OD	OS	OD	OS
G	103.3 ± 8.5	102.6 ± 8.6	101.6 ± 8.4	100.9 ± 8.1	0.33	0.30
N	62.6 ± 10.3	58.9 ± 9.8	59.5 ± 10.7	57.8 ± 9.5	0.15	0.55
NS	100.0 ± 17.0	98.5 ± 17.9	100.5 ± 15.8	101.3 ± 14.8	0.88	0.43
TS	146.3 ± 18.1	145.9 ± 14.4	142.1 ± 14.3	142.6 ± 14.6	0.22	0.27
T	81.6 ± 11.0	85.1 ± 10.7	80.3 ± 10.3	82.3 ± 10.8	0.53	0.20
TI	165.4 ± 16.9	168.5 ± 16.0	165.1 ± 17.1	164.3 ± 16.1	0.92	0.20
NI	125.6 ± 20.5	119.5 ± 23.4	125.0 ± 22.0	117.9 ± 19.4	0.89	0.72

Data are presented as mean ± standard deviation. *P*-values represent comparison of females versus males for right and left eyes.

OD, right eye; OS, left eye; G, global; N, nasal; NS, nasal superior; TS, temporal superior; T, temporal; TI, temporal inferior; NI, nasal inferior.

CDR >0.5 or disc hemorrhage based on inspection of FP, diffuse or focal narrowing of the RNFL or the neuroretinal rim (especially in the superior or inferior sector of the optic disc) based on slit lamp biomicroscopic optic nerve examination. Further evaluation considered OCT quantification of CDR values and RNFL thickness, in which circumpapillary OCT showed diffuse or focal arcuate thinning ($P < 0.01$ in one OCT examination or $P < 0.05$ in two OCT examinations that were carried out six months apart) compared to the normative database. An example of the OCT output from a 15-year-old male glaucoma suspect with conscious IOP of 20 mm Hg OD and 22 mm Hg OS is provided in Figure 5. Glaucoma suspects had similar age, body weight, and FPG levels compared with the control group ($P = 0.41$) but had borderline higher fasting triglyceride levels ($P = 0.06$). Suspects displayed significantly higher conscious IOP (16.2 ± 3.9 vs. 13.9 ± 2.1 mm Hg; $P = 0.001$) and CDR values compared to the control group (0.59 ± 0.06 vs. 0.36 ± 0.08; $P = 5.66E\text{-}30$; Table 3). Interestingly, only four of 18 glaucoma suspects (or 5 of 31 eyes suspects of glaucoma) showed a conscious IOP >21 mm Hg, whereas four of the 108 control monkeys (six of 216 eyes) had a conscious IOP >21 mm Hg. All sectors (except the temporal sector) on the circumpapillary OCT revealed significant reduction in RNFL thickness in glaucoma suspects compared to controls after adjustment for multiple comparisons ($P \leq 0.0022$; Table 4). All glaucoma suspect monkeys had unremarkable slit lamp examinations and open angles based on anterior segment OCT (Supplementary Fig. S1). RNFL defects were absent based on inspection of fundus photographs (Fig. 6A) from controls but were almost invariably present in glaucoma suspects (Fig. 6B).

The baseline differences in OCT thicknesses between glaucoma suspects and normal monkeys were not merely related to aging. We compared OCT parameters between young (mean age: 10.3 ± 1.7 years; n = 30 monkeys) and old normal monkeys (mean age: 20.6 ± 1.4 years; n = 20 monkeys) and evaluated right and left eye differences for the seven OCT parameters (Supplemental Table S1). Despite the marked difference in age (30 vs. 60 in human chronological years), only global RNFL thickness for the right eye (103.1 ± 5.6 μm vs. 99.0 ± 6.4 μm for young and old respectively; $P = 0.02$) and temporal sector RNFL thickness for the left eye (86.2 ± 12.1 μm vs. 78.0 ± 12.1 μm for young and old, respectively; $P = 0.02$) showed nominal age related declines. In contrast, the glaucoma suspects (mean age 14.7 ± 4.0 years; n = 15) had marked reductions in six of seven baseline OCT parameters in at least one eye compared to the old controls (mean age: 20.6 ± 1.4 years; n = 20 monkeys) after correcting for multiple comparisons made on an eye for eye basis ($P \leq 0.006$, Supplementary Table S2). The reductions in these OCT parameters were present despite the significantly younger age of glaucoma suspects (Supplementary Table S2).

Progressive Retinal Neuron Damage in Longitudinal Studies of Glaucoma Suspects

To further investigate whether glaucoma suspects underwent progressive optic nerve damage, we performed three-year longitudinal analysis of FP and OCT assessments from 15 (11 males and 4 females) of the 18 glaucoma suspects. Three of the seven female glaucoma suspects were kept in the breeding colony and thus did not participate in the three-year follow-up. In addition, 40 age- and sex-matched healthy controls

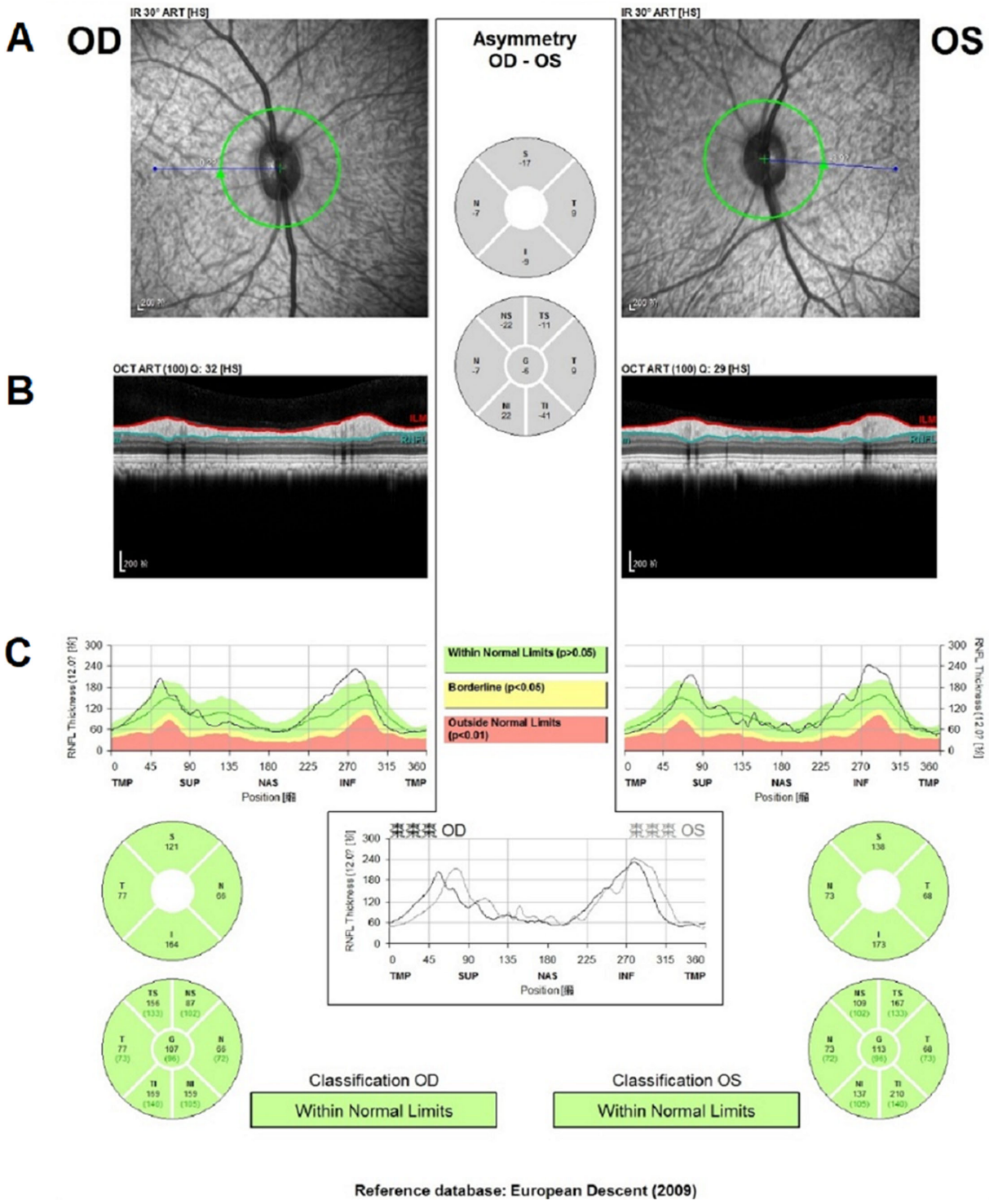

Figure. 4. Representative case of SD-OCT assessment for RNFL thickness in a 19-year-old female Rhesus monkey not regarded as a glaucoma suspect. Representative circular scans from the center of optic nerve head (**A**) and RNFL circular cut images (**B**) of the right (*OD*) and left (*OS*). **C.** The spectralis RNFL circular profile with comparisons to an age matched human control of comparable chronological age (57 years).

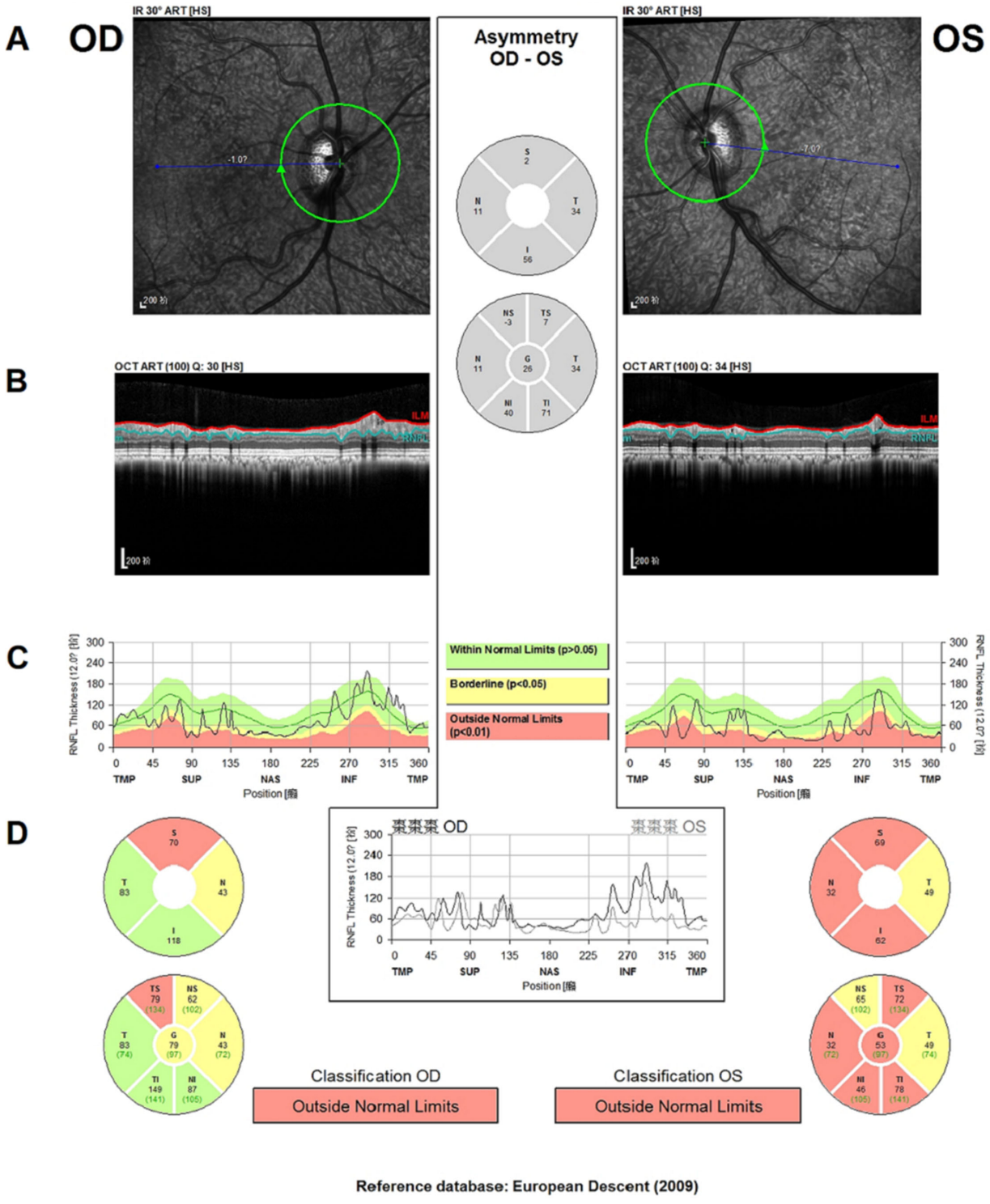

Figure 5. SD-OCT assessment of RNFL thickness in a 15-year-old male glaucoma suspect Rhesus monkey with IOP of 20 mm Hg OD and 22 mm Hg OS. Representative circular scans from the center of optic nerve head **(A)** and Spectralis RNFL circular cut images (**B**) of both eyes. Note the enlarged cups in both eyes. **(C)** The Spectralis RNFL thickness map and RNFL thickness deviation map highlight the clock hours of peripapillary RNFL that is outside normal limits compared to an age-matched human controls with comparable chronological age (45 years). (**D)** A localized superior RNFL defect is present OD and a diffuse RNFL defect is present OS.

Table 3. Baseline Characteristics of Glaucoma Suspects and the Control Group

Group (n = Male/Female)	Control (n = 70/38)	Glaucoma Suspects (n = 11/7)	*P* Value
Age (y)	14.6 ± 2.0	14.3 ± 4.1	0.64
Body weight (kg)	9.3 ± 2.2	9.7 ± 2.2	0.52
Systolic blood pressure (mm Hg)	130.4 ± 15.0	129.7 ± 19.4	0.87
Diastolic blood pressure (mm Hg)	64.7 ± 8.4	65.8 ± 10.4	0.62
Fasting plasma glucose (mg/dL)	83.0 ± 14.9	86.5 ± 24.2	0.41
Triglycerides (mg/dL)	0.49 ± 0.16	0.58 ± 0.31	0.06
Conscious IOP (mm Hg)			
OD	13.9 ± 2.3	16.2 ± 3.5	0.001*
OS	13.9 ± 2.4	16.3 ± 4.4	0.002*
CDR	0.36 ± 0.08	0.59 ± 0.06	5.66E-30*

Data are presented as mean ± SD; *P* values represent comparison of glaucoma suspects versus controls.
*Statistically significant differences by Student's *t* test.

Table 4. Comparison of Baseline Retinal Nerve Fiber Layer Parameters Of The Glaucoma Suspect and Control Group

	Controls (n = 70/38)		Glaucoma Suspects (n = 11/7)		*P* Value	
Group (n = Male/Female)	OD	OS	OD	OS	OD	OS
G	102.7 ± 8.5	102.0 ± 8.4	91.5 ± 11.0	86.7 ± 15.0	4.8E-06*	1.0E-07*
N	61.5 ± 10.5	58.5 ± 9.7	52.0 ± 8.4	48.5 ± 10.6	6.0E-04*	5.4E-04*
NS	100.2 ± 16.6	99.5 ± 16.9	86.7 ± 15.1	83.7 ± 20.5	2.2E-03*	1.9E-03*
TS	144.8 ± 17.0	144.8 ± 14.6	129.5 ± 19.9	125.0 ± 29.7	1.1E-03*	8.8E-05*
T	81.1 ± 10.8	84.2 ± 10.8	82.1 ± 10.1	78.1 ± 17.5	0.73	0.07
TI	165.3 ± 16.9	167.0 ± 16.2	144.9 ± 35.3	136.7 ± 30.2	2.3E-04*	6.4E-08*
NI	125.4 ± 21.0	119.0 ± 22.0	102.2 ± 24.0	95.3 ± 25.8	7.0E-05*	3.6E-04*

Data are presented as mean ± standard deviation averaged from the baseline measurements. *P*-values represent comparison of glaucoma suspects versus controls for right and left eyes.
*Statistically significant differences by student *t* test.
OD, right eye; OS, left eye; RNFL, retinal nerve fiber layer; G, global; N, nasal; NS, nasal superior; TS, temporal superior; T, temporal; TI, temporal inferior; NI, nasal inferior.

(30 males and 10 females) from the 108 controls were selected to participate in the longitudinal study. Although some monkeys in the large cohort (N = 722) needed treatment for severe hypertension during the three-year period, none of the glaucoma suspects or the 40 healthy controls was classified as severe hypertension. One of the 40 controls was classified as having severe diabetes mellitus and treated with insulin.

OCT quantification of RNFL thickness (Fig. 7) and fundus photomicrographs (Fig. 8) both detected definite progressive RNFL thinning over a three-year period. The CDR and OCT parameters in the control group remained constant during the three-year period ($P \geq 0.09$), whereas the glaucoma suspect group showed significant increased CDR value ($P = 0.02$) and nominally significant reduction of the nasal ($P = 0.02$) and nasal superior RNFL thickness ($P = 0.046$) at year 3, indicating progressive optic nerve damage (Table 5 and Supplementary Tables S3 and S4). The average conscious IOP of the glaucoma suspect group (15.4 ± 3.2 mm Hg) was significantly higher than the control group (12.8 ± 4.4 mm Hg; $P = 0.004$) throughout the period of three years' follow-up, but no significant escalation of IOP from baseline was detected ($P \geq 0.60$).

Central Nervous System Neuroimaging Results

T1-weighted and T2 flair MRI on a male glaucoma suspect (age 16) and a male normal monkey (age 15) depicted in Figure 6 revealed no chiasmal or central system abnormalities (Supplementary Fig. S2).

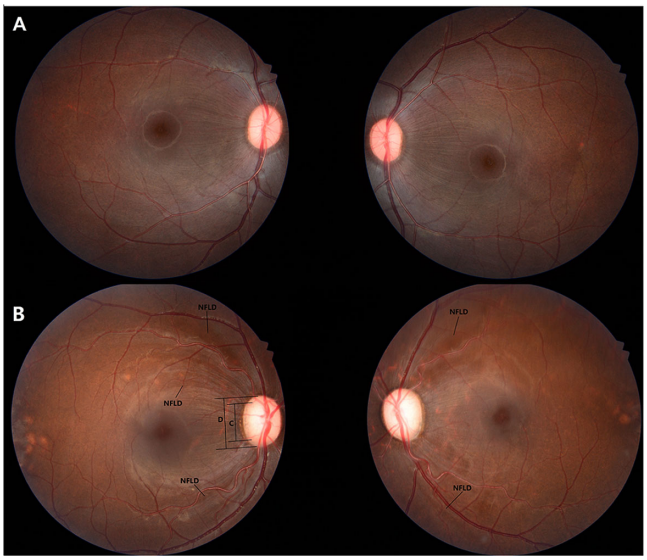

Figure 6. Fundus images of Rhesus monkeys. **(A)** Representative fundus photos of right and left eyes of a 15-year-old normal male monkey with IOP of 13 mm Hg OD and 10 mm Hg OS. (**B**) Fundus photos of right and left eyes of a 16-year-old male glaucoma suspect with IOP of 23 mm Hg OD and 24 mm Hg OS. NFLD, nerve fiber layer defect; C, cup; D, disc.

Discussion

In this study 18 of 722 rhesus monkeys (2.5%) were regarded as glaucoma suspects and had higher baseline conscious IOP compared to age-matched controls (16.2 mm Hg vs. 13.9 mm Hg; $P \leq 0.002$). Interestingly, only four of 18 glaucoma suspects showed a conscious IOP >21 mm Hg, whereas four of the 108 control monkeys had a conscious IOP >21 mm Hg. Previously a glaucomatous optic nerve phenotype across the spectrum of IOP has been described in a closed colony located off the coast of Puerto Rico.[13,20] In our closed Chinese colony, we undertook a systematic approach to identify all glaucoma suspects using an optic nerve-based screening approach and we documented progressive RNFL thinning and increased cupping based on OCT measurements taken over three years in monkeys regarded as glaucoma suspects at baseline. We present data supporting the notion that optic nerve findings in the glaucoma suspects were not merely age related (Supplementary Tables S1 and S2). Glaucoma suspects and controls had normal slit lamp examinations and open angles on anterior segment OCT. IOP did not increase over a three-year follow-up period in glaucoma suspects and controls. MRIs showed no secondary cause for optic nerve degeneration in two monkeys (one suspect and one control; Supplementary Fig. S2).

It is becoming increasingly recognized that elevated IOP >21 mm Hg is not a good biomarker for new onset of human glaucoma. In Barbados[21] and Melbourne Australia,[22] roughly 75% and 50% of incident open-angle glaucoma respectively had baseline IOP <21 mm Hg. Birth cohort studies represent another strategy to capture IOP data in newly recognized untreated glaucoma. In the 1966 Birth Cohort Study performed in Northern Finland, a point estimate of IOP in glaucoma eyes was only 15.9 mm Hg vs. 14.9 in nonglaucomatous eyes (95% of the glaucoma eyes were untreated).[23] Only a minority of OAG in this birth cohort had IOP >21 mm Hg (11%). These data mimic the baseline IOP profile of glaucoma suspects in our cohort, suggesting this colony at risk for glaucoma offers opportunities to understand the mechanisms underlying optic nerve vulnerability in POAG.

The optic nerve head is the target of disease in POAG but it is surprisingly challenging to find a consensus definition of POAG as has been previously noted.[24] With the advent of OCT imaging of the optic nerve and RNFL a definition of glaucomatous deterioration incorporating a temporal component seems essential. In fact our study provides suggestive evidence that selected OCT parameters were declining over time in a statistically significant manner, but even these findings were not significant after adjusting for multiple comparisons, probably due to the sample size (15 suspects and 40 controls) and relatively short follow-up period (three years). It is known that progressive global RNFL loss in human POAG is slow (typically <1 µm/y).[25] In fact the progressive changes mostly in the nasal aspect of the disc prompted us to perform post hoc neuroimaging that revealed no chiasmal lesions.

Collectively our glaucoma suspect monkeys experienced an increase in CDR and significant thinning of the nasal and nasal superior RNFL sectors on OCT in three years of follow-up. Thus, although it is true that OCT platforms do not have normative monkey data, when compared to themselves over time, the glaucoma suspects experienced loss of neuronal tissue, and the controls did not. The fundus photos showed that loss of the RNFL reflex along the superior and inferior retinal vascular arcades on fundus photos of glaucoma suspects but this manifested as progressive loss on the nasal sectors with OCT. The reason why the OCT seemed to show progressive loss in the nasal region is an artifact of OCT testing in adult rhesus monkey eyes whose mean axial length is 17 mm versus 23 mm in humans.[26] The relative hyperopia of monkey eyes causes a concentration of nerve fiber layer axons in the nasal sectors. The nerve fiber bundles tend to concentrate along the vascular arcades which are located

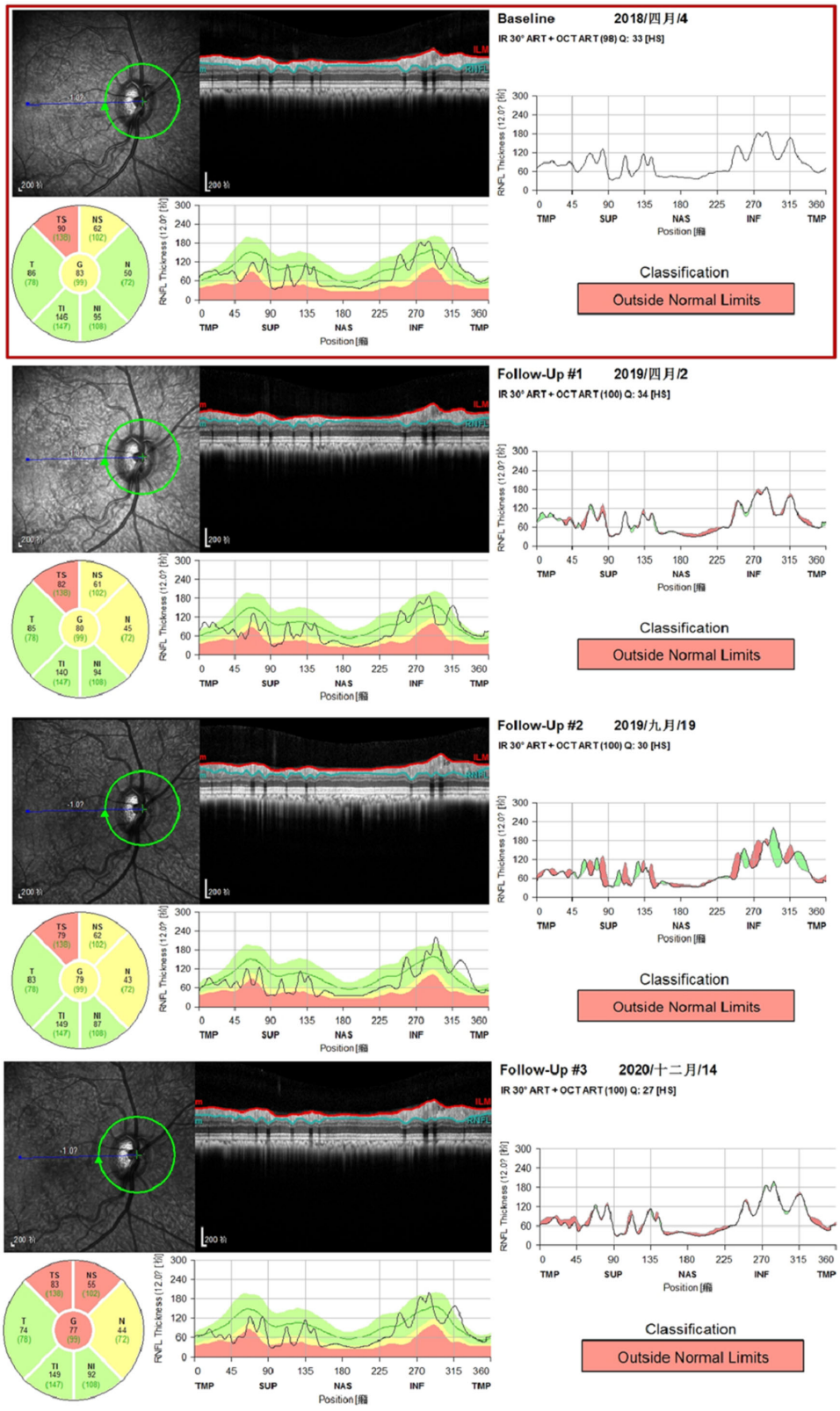

Figure 7. Progressive RNFL thinning in a glaucoma suspect monkey by SD-OCT assessments. OCT serial report ranging from 2018 to 2020 showing progressive thinning in the superior temporal quadrant. The OCT was taken from a 16-year-old male glaucoma suspect monkey with IOP at 20 mm Hg OD and 23 mm Hg OS in year 1 and 20 mm Hg OD and 21 mm Hg OS in year 3.

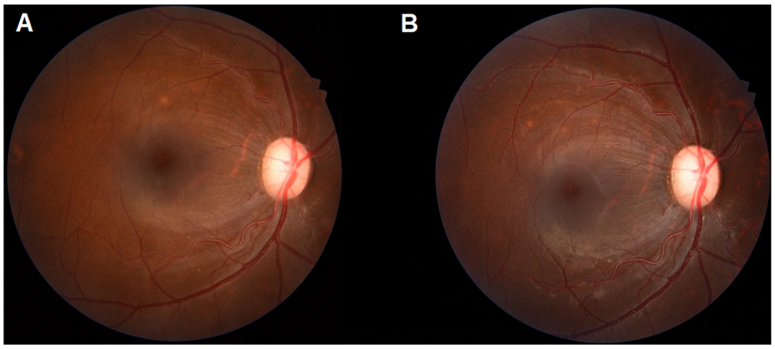

Figure 8. Progressive loss of nerve fibers shown in fundus images of a glaucoma suspect monkey. Representative fundus photos of right eye of a male glaucoma suspect monkey taken on July 20, 2017 (**A**), and September 19, 2019 (**B**).

more temporally in myopic eyes[27] and more nasally in hyperopic eyes.[28] We also provide confirmation that progressive RNFL loss occurred on serial fundus photographs (Fig. 8). Estimation of cupping (Fig. 5) and change in cupping from fundus photos (Fig. 8) can be challenging; hence, OCT is essential to following disease in this animal model.

This work indicates that these monkeys are an excellent model to understand what makes optic nerves susceptible to IOPs that are only slightly higher than monkeys who do not develop progressive optic neuropathy. Metabolic derangements, as well as genetic factors are obvious candidate factors for this deterioration. In our sample we did not notice obvious derangement in blood pressure and fasting blood sugar, although fasting triglycerides were slightly higher in glaucoma suspects. Larger sample sizes are needed to assess metabolic factors that might be linked to optic nerve structure. Rare (*TBK1*[29] and *OPTN*[30]) and common variants (*CDKN2B-AS*)[31,32] are among the many candidate genes for optic nerve susceptibility in this closed colony, and we are currently collecting DNA and constructing pedigrees that will allow for such analyses. It is likely that there is high homology between these, and other glaucoma candidate genes between rhesus monkeys and humans, as has already been demonstrated for *TBK1*.[33]

Table 5. Comparisons of Cup Disc Ratio, Intraocular Pressure (mm Hg) and RNFL Parameters (μm) at Baseline and During Three-Year Follow-Up of Glaucoma Suspects and Control Monkeys

	Controls (n = 30 Male/ 10 Female)			Glaucoma Suspects (n = 11 Male/4 Female)		
Group (n = Male/Female)	Baseline	Year 3	*P* Value	Baseline	Year 3	*P* Value
CDR	0.39 ± 0.07	0.39 ± 0.08	0.90	0.59 ± 0.06	0.66 ± 0.09	0.02*
IOP						
OD	13.3 ± 4.3	13.2 ± 4.6	0.87	15.5 ± 3.0	14.9 ± 2.7	0.60
OS	12.4 ± 3.9	12.5 ± 4.0	0.90	15.5 ± 4.0	15.9 ± 3.9	0.80
G	103.7 ± 5.5	103.8 ± 6.0	0.91	85.5 ± 11.6	79.2 ± 12.6	0.08
N	61.4 ± 8.3	60.6 ± 7.9	0.57	48.8 ± 9.8	43.1 ± 7.7	0.03*
NS	106.7 ± 14.1	103.1 ± 12.7	0.093	82.3 ± 16.9	72.6 ± 14.6	0.04*
TS	148.0 ± 12.5	147.9 ± 12.6	0.94	122.7 ± 24.9	113.2 ± 24.1	0.19
T	80.4 ± 10.6	80.9 ± 10.5	0.77	77.4 ± 13.6	76.4 ± 19.1	0.84
TI	167.6 ± 14.6	168.1 ± 15.0	0.82	132.8 ± 31.3	121.1 ± 40.8	0.27
NI	123.7 ± 19.1	127.9 ± 18.0	0.16	94.4 ± 23.0	87.2 ± 25.4	0.31

Data are presented as mean ± SD. A total of 25 eyes of the 15 glaucoma suspects and 60 eyes of 30 controls were used for statistical analysis. When available, each monkey is represented by the average of CDR and OCT parameters from both eyes. *P*-values represent comparison of baseline versus year 3.

*Statistically significant differences by Student's *t* test.

CDR, cup disc ratio; IOP, intraocular pressure; G, global; N, nasal; NS, nasal superior; TS, temporal superior; T, temporal; TI, temporal inferior; NI, nasal inferior.

This work has notable weaknesses and strengths. Weaknesses include the fact that we did not measure outflow facility in these animals, although we did note the angles were open on gonioscopy and anterior segment OCT in glaucoma suspects (Supplementary Fig. S1). We did not document functional visual loss in glaucoma suspects because that was beyond the scope of this project. The number of monkeys with suspect glaucoma was small but the burden of disease in this population is comparable to the global prevalence of POAG.[34] We did not measure central corneal thickness in these monkeys, but that is unlikely to alter the IOP profile in this colony. We performed only limited neuroimaging to rule out central nervous system disease, but it is clear that glaucoma suspect monkeys presented with bilateral optic nerve disease manifesting as enlargement of CDR and evolving NFL defects. Thus it is unlikely there would be a localizing central nervous system lesion to explain these defects. Interesting neuroimaging was performed on selected monkeys in the Cayo Santiago colony with open-angle glaucoma at "normal IOP" and those studies were negative. A strength of our study was the systematic optic nerve-based approach to screen the colony that was not biased by IOP levels. The strategy was driven by the use of clinical optic nerve evaluation, fundus photographs, and OCT. Also, these animals had systemic evaluation for hypertension and diabetes and future research will assess whether these conditions contribute to glaucoma in this colony. Finally, we followed suspects and controls for three years and documented progressive optic nerve deterioration in suspects, although longer follow-up is needed.

In conclusion we report that a Chinese colony of rhesus monkeys under careful surveillance demonstrate salient features of POAG; namely, the monkeys had open angles and no signs of anterior segment dysgenesis but progressive optic nerve deterioration. The IOP in cases was higher than controls suggesting the glaucoma was IOP-related but clearly other optic nerve vulnerability factors may be at play. Clearly, a higher level of IOP and blood pressure profiling, such as was performed by Wilson et al.[35] is in order in these monkeys. Overall, they represent an unprecedented opportunity to study the natural history and pathogenesis of POAG.

Acknowledgments

Supported by funding from the PriMed Non-human Primate Research Center of Sichuan PriMed Shines Bio-tech Co., Ltd. Louis R. Pasquale is supported in part by an unrestricted challenge grant from Research to Prevent Blindness (New York City).

Disclosure: **L.R. Pasquale**, Twenty twenty (C), Nicox (C), Skye Biosciences (C), Eyenovia (C); **L. Gong**, PriMed (E, S); **J.L. Wiggs**, Allergan (C), Editas (C), Maze (C), Regenxbio (C), Aerpio Pharmaceuticals (F); **L. Pan**, PriMed (E); **Z. Yang**, PriMed (E); **M. Wu**, PriMed (E); **Z. Yang**, PriMed (E); **D.F. Chen**, Boston Pharma (C), i-Lumen (C), PriMed (C), Massachusetts Eye and Ear (P); **W. Zeng**, PriMed (E, S)

References

1. Iyer J, Vianna JR, Chauhan BC, Quigley HA. Toward a new definition of glaucomatous optic neuropathy for clinical research. *Curr Opin Ophthalmol*. 2020;31(2):85–90.
2. Wilson MR, Kosoko O, Cowan CL, Jr, Sample PA, Johnson CA, Haynatzki G, Enger C, Crandall D. Progression of visual field loss in untreated glaucoma patients and glaucoma suspects in St. Lucia, West Indies. *Am J Ophthalmol*. 2002;134(3):399–405.
3. Leske MC, Heijl A, Hyman L, Bengtsson B. Early Manifest Glaucoma Trial: design and baseline data. *Ophthalmology*. 1999;106(11):2144–2153.
4. Anderson DR, Drance SM, Schulzer M, Collaborative Normal-Tension Glaucoma Study Group. Natural history of normal-tension glaucoma. *Ophthalmology*. 2001;108(2):247–253.
5. Pang IH, Clark AF. Inducible rodent models of glaucoma. *Prog Retin Eye Res*. 2020;75:100799.
6. Morrison JC, Cepurna WO, Johnson EC. Modeling glaucoma in rats by sclerosing aqueous outflow pathways to elevate intraocular pressure. *Exp Eye Res.* 2015;141:23–32.
7. Morgan JE, Tribble JR. Microbead models in glaucoma. *Exp Eye Res.* 2015;141:9–14.
8. Overby DR, Clark AF. Animal models of glucocorticoid-induced glaucoma. *Exp Eye Res.* 2015;141:15–22.
9. Morrison JC, Cepurna WO, Tehrani S, et al. A period of controlled elevation of IOP (CEI) produces the specific gene expression responses and focal injury pattern of experimental rat glaucoma. *Invest Ophthalmol Vis Sci.* 2016;57(15):6700–6711.
10. Jain A, Zode G, Kasetti RB, et al. CRISPR-Cas9–based treatment of myocilin-associated glaucoma. *Proc Natl Acad Sci USA*. 2017;114(42):11199–11204.

11. Kasetti RB, Maddineni P, Kiehlbauch CC, et al. Autophagy stimulation reduces ocular hypertension in murine glaucoma model via autophagic degradation of mutant myocilin. *JCI Insight*. 2021;4:143359.
12. Burgoyne CF. The non-human primate experimental glaucoma model. *Exp Eye Res*. 2015;141:57–73.
13. Dawson WW, Brooks DE, Hope GM, et al. Primary open angle glaucomas in the rhesus monkey. *Br J Ophthalmol*. 1993;77(5):302–310.
14. Takada N, Omodaka K, Kikawa T, et al. OCT-based quantification and classification of optic disc structure in glaucoma patients. *PLoS One*. 2016;11(8):e0160226.
15. Mattison JA, Vaughan KL. An overview of nonhuman primates in aging research. *Exp Gerontol*. 2017;94:41–45.
16. Crowston JG, Hopley CR, Healey PR, Lee A, Mitchell P; Blue Mountains Eye Study. The effect of optic disc diameter on vertical cup to disc ratio percentiles in a population based cohort: the Blue Mountains Eye Study. *Br J Ophthalmol*. 2004;88(6):766–770.
17. Andrade MC, Ribeiro CT, Silva VF, et al. Biologic data of Macaca mulatta, Macaca fascicularis, and Saimiri sciureus used for research at the Fiocruz primate center. *Mem Inst Oswaldo Cruz*. 2004;99(6):581–589.
18. Nakatani Y, Higashide T, Ohkubo S, Takeda H, Sugiyama K. Evaluation of macular thickness and peripapillary retinal nerve fiber layer thickness for detection of early glaucoma using spectral domain optical coherence tomography. *J Glaucoma*. 2011;20(4):252–259.
19. Alasil T, Wang K, Keane PA, et al. Analysis of normal retinal nerve fiber layer thickness by age, sex, and race using spectral domain optical coherence tomography. *J Glaucoma*. 2013;22(7):532–541.
20. Dawson WW, Brooks DE, Dawson JC, Sherwood MB, Kessler MJ, Garcia A. Signs of glaucoma in rhesus monkeys from a restricted gene pool. *J Glaucoma*. 1998;7(5):343–348.
21. Leske MC, Connell AM, Wu SY, et al. Incidence of open-angle glaucoma: the Barbados Eye Studies. The Barbados Eye Studies Group. *Arch Ophthalmol*. 2001;119(1):89–95.
22. Mukesh BN, McCarty CA, Rait JL, Taylor HR. Five-year incidence of open-angle glaucoma: the visual impairment project. *Ophthalmology*. 2002;109(6):1047–1051.
23. Karvonen E, Stoor K, Luodonpää M, et al. Prevalence of glaucoma in the Northern Finland Birth Cohort Eye Study. *Acta Ophthalmol*. 2019;97(2):200–207.
24. Kroese M, Burton H. Primary open angle glaucoma. The need for a consensus case definition. *J Epidemiol Community Health*. 2003;57(9):752–754.
25. Hou H, Shoji T, Zangwill LM, et al. Progression of Primary Open-Angle Glaucoma in Diabetic and Nondiabetic Patients. *Am J Ophthalmol.* 2018;189:1–9.
26. Wiesel TN, Raviola E. Increase in axial length of the macaque monkey eye after corneal opacification. *Invest Ophthalmol Vis Sci.* 1979;18(12):1232–1236
27. Yamashita T, Kii Y, Tanaka M, et al. Relationship between supernormal sectors of retinal nerve fibre layer and axial length in normal eyes. *Acta Ophthalmol.* 2014;92(6):e481–e487.
28. Dikkaya F, Erdur SK. Comparison of optical coherence tomography measurements between high hyperopic and low hyperopic children. *Ther Adv Ophthalmol.* 2020;12:1–10.
29. Awadalla MS, Fingert JH, Roos BE, et al. Copy number variations of TBK1 in Australian patients with primary open-angle glaucoma. *Am J Ophthalmol*. 2015;159(1):124–130.e1.
30. Aung T, Rezaie T, Okada K, et al. Clinical features and course of patients with glaucoma with the E50K mutation in the optineurin gene. *Invest Ophthalmol Vis Sci*. 2005;46(8):2816–2822.
31. Pasquale LR, Loomis SJ, Kang JH, et al. *CDKN2B-AS1* genotype-glaucoma feature correlations in primary open-angle glaucoma patients from the United States. *Am J Ophthalmol*. 2013;155(2):342–353.e5.
32. Burdon KP, Crawford A, Casson RJ, et al. Glaucoma risk alleles at CDKN2B-AS1 are associated with lower intraocular pressure, normal-tension glaucoma, and advanced glaucoma. *Ophthalmology*. 2012;119(8):1539–1545.
33. Rezaie T, Waitzman DM, Seeman JL, Kaufman PL, Sarfarazi M. Molecular cloning and expression profiling of optineurin in the rhesus monkey. *Invest Ophthalmol Vis Sci*. 2005;46(7):2404–2410.
34. Tham YC, Li X, Wong TY, Quigley HA, Aung T, Cheng CY. Global prevalence of glaucoma and projections of glaucoma burden through 2040: a systematic review and meta-analysis. *Ophthalmology*. 2014;121(11):2081–2090.
35. Wilson KI, Godara P, Jasien JV, et al. Intra-subject variability and diurnal cycle of ocular perfusion pressure as characterized by continuous telemetry in nonhuman primates. *Invest Ophthalmol Vis Sci.* 2020;61(6):7.